Experimental Thermal and Fluid Science 53 (2014) 57–69

Contents lists available at ScienceDirect

Experimental Thermal and Fluid Science

journal homepage: www.elsevier.com/locate/etfs

Bubbly structures in a cavitating slot orifice

Matjaž Perpar *, Erazem Polutnik, Marko Pečar, Iztok Žun

Laboratory for Fluid Dynamics and Thermodynamics, Faculty of Mechanical Engineering, University of Ljubljana, Aškerčeva 6, 1000 Ljubljana, Slovenia

ARTICLE INFO

Article history:
Received 17 July 2013
Received in revised form 1 November 2013
Accepted 3 November 2013
Available online 23 November 2013

Keywords:
Cavitation
Visualization
Local phase detection
Local pressure measurements
Bubbly flow regimes

ABSTRACT

The research refers to the experimental study of cavitation phenomena when water was passing through the slot orifice. The contribution brought up by this article is the detailed time and space dependent analysis of bubbly structures identified using high speed video, microresistivity probes, optical fibre pressure probe, and hot film probe. Two principle experiments were carried out to study cavitation in a confined geometry. The first one was designed to study an induced single bubble cavitation when the water pressure was reduced below the atmospheric pressure, but was still high enough so that there was not any saturated pressure in the slot region. The second experiment was undertaken at a reference pressure which was sufficient to produce a massive cavitation in the slot region. The following flow regimes were identified and analyzed in detail: the so-called detachment regime where bubble breakup was observed in the case of the individual bubble cavitation; and in the case of the large scale cavitation, the regime of macroscopic bubbles clustering into bubble cloud and the regime of collapsing bubbles.

1. Introduction

Our research refers to the experimental study of bubbly structures caused by cavitation in water flow through a slot orifice. Cavitation in a confined geometry remains a consistent design problem in various engineering frontiers. Orifices are often used to investigate this phenomenon because they provide an easy way to meet the fundamental requirement for cavitation to occur, i.e. a sufficient reduction in the static pressure. In addition, the orifice represents a typical example of contraction in the hydraulic system where the cavitation is interesting from the viewpoints of the fluid performance, noise and erosion.

Over the last two decades, much effort has been invested to explain cavitation structures in orifice flows, with considerable emphasis on the scale effects [1–4]. However, the details that describe a particular cavitating flow pattern, like cloud cavitation for example, are not sufficient to provide the needed data for numerical simulation on meso and micro scales at the same time. Bubbles that have eventually clustered into a cloud are usually not understood either by size or by number density. Also the transient characteristics of clouds that bubbles are forming are unknown. Many times impact rates are calculated based on the postulated Raileigh Plesset equation that has been derived in relation to a single spherical bubble.

Cavitating flow patterns in orifices were usually observed at high liquid velocities, for instance 10–18 m/s in conventional orifices with an internal diameter of 15–30 mm [1,2] or within 18 and 28 m/s in the micro-orifice with an 11.5 μm square throat [3]. Since detailed observation of the cavitation mechanism is more successful at lower liquid velocities [5], our experiment was designed to provide a liquid velocity in the slot at around 3.5 m/s. Lower fluid velocity is especially needed to observe the cavitation inception more accurately, because the cavitation nuclei require a finite residence time to grow to observable size [6]. The aim of the present work is to provide sufficient experimental data to be able to validate numerical simulation. In this context, it is crucial to search for the indicators that play a major role in the cavitation process. For practical purposes, it is useful to distinguish [7]: the *limiting regime* between the non-cavitating flow and the cavitating flow and the *regime of developed cavitation*. In the case of limiting regime, the *threshold of cavitation inception or cavitation disappearance* is of interest, while in the second case, assuming that this threshold is overstepped, the consequences of cavitation on the operation of the hydraulic system in question.

High speed video is a common technique used for observing the cavitation process. Besides monitoring the flow structures, the grey level analysis of images enables the obtainment of the frequency spectrum of the gas phase fluctuations [4,8–10]. For the applications where transparent walls can't be used, accelerometers were successfully applied to characterize the cavitation dynamics [2,11]. Additionally, cavitation noise measurements outside the piping were performed to detect the various cavitation states [12]. This method can be especially useful in cases where hot liquids are applied. Since phase fraction is an important emergent parameter of two phase flow, much effort has been devoted to void fraction measurements during cavitation. The X-ray attenuation technique was found suitable for describing the cavitation

* Corresponding author. Tel.: +386 1 47 71 419; fax: +386 1 47 71 447.
E-mail address: matjaz.perpar@fs.uni-lj.si (M. Perpar).

0894-1777/$ - see front matter © 2013 Elsevier Inc. All rights reserved.
http://dx.doi.org/10.1016/j.expthermflusci.2013.11.003

structures at meso scale [13,14]. The X-ray CT measurements [15] enabled local but time-averaged void fraction distribution within the cavitating flow. Local void fraction and liquid velocity fields can be obtained through magnetic resonance imaging, as has been shown for the case of acoustic cavitation [16]. LDV [10] and PIV techniques [17] were also found applicable for velocity measurements in cavitating liquids. Since the vapour bubbles act as additional tracers in the system, it is necessary to take into account the cavitation structure and measurement of uncertainty to obtain reasonable results utilizing the PIV technique [17]. Today, X-ray absorption and PIV techniques are two of the best possible choices to obtain void fraction and velocity fields in cavitating flows, but they are very expensive. On the other hand, the use of a double optical probe [18,19] is a very cheap method to obtain accurate data on both void fraction and velocity fields.

In our experiment, due to reduced static pressure in the vacuum chamber, the cavitation structures not only occurred in the slot [20,21] but also outside it. The contribution brought up by this article is the detailed time and space dependent analysis of bubbly structures based on different measurement techniques. High speed video was used to observe the transient characteristics of bubble structures and bubble cloud formation, i.e. its growth and collapse. Based on digital image processing, cloud impact rate on a solid surface, bubble time scale estimate and bubble cloud life span were evaluated. The statistical relevance of bubble structures has been checked by taking double microresistivity probe measurements including bubble number density, bubble generation frequency, void fraction, bubble velocity and the bubble length scale estimate. Bubble cloud morphology was investigated via synchronized records of video images and resistivity probe signals. A micro optical pressure probe was used to analyse the liquid bulk dynamics. The details are shown on the individual bubble breakup, on bubble cloud dynamics and on the background of bubble impact rate. The latter was important in the modelling of the cavitation erosion process that was the subject of collaboration with AVL List GmbH within the EU project PREVERO.

2. Experiment

2.1. Experimental set-up

A closed loop to run water under controlled flow parameters has been constructed as shown in Fig. 1. The vacuum chamber (A) with 170 mm side length preserved a very stable low pressure field. Water is pumped by a circulation pump (B) through the rotameter (6) with a vertical draft pipe of ID/OD = 14/20 mm, and through the concentrical slot, see details in Fig. 1. The slot width was adjusted in this case by the flat plug positioned above the draft pipe exit to 1.4, 1.5 and 1.6 mm. The additional pressure drop due to the flow of water through the confined passage produced cavitation that could be perceived by AVL FIRE code simulation. A constant water level (245–250 mm above the slot) in the vacuum chamber was maintained. At this level, the saturation pressure at room temperature was provided by the vacuum pump (C). The condenser (D), cooled by tap water, was used to prevent vapour entry in the vacuum pump. A probe traversing system (E) enabled point probe positioning at a minimal step of 10 μm. The following probes were used (optionally): double resistivity probe (1), optical pressure probe (2) or constant temperature anemometer (CTA) probe (3).

The cavitation process was controlled by temperature (4) and pressure (5) measurements. Temperature was obtained by a type K thermocouple connected to a *Greisinger* GTH 1200 digital thermometer with 0.1 °C resolution in the −65 to 199.9 °C range. An in-house constructed thermocouple (with 1 mm probe tip diameter) was tested within a range of 10 °C and 25 °C, the accuracy was ±0.4 °C. To get the absolute pressure in the vacuum chamber, vacuum and atmospheric pressure were measured using a GDH 13 AN differential manometer (range 0–1999 mbar, resolution 1 mbar) and *Greisinger* GPB 1300 barometer (300–1100 mbar, resolution 1 mbar). Considering the typical accuracy of the differential manometer (±1 mbar) and barometer (±2 mbar), the accuracy of the absolute pressure measurements was estimated to be ±3 mbar.

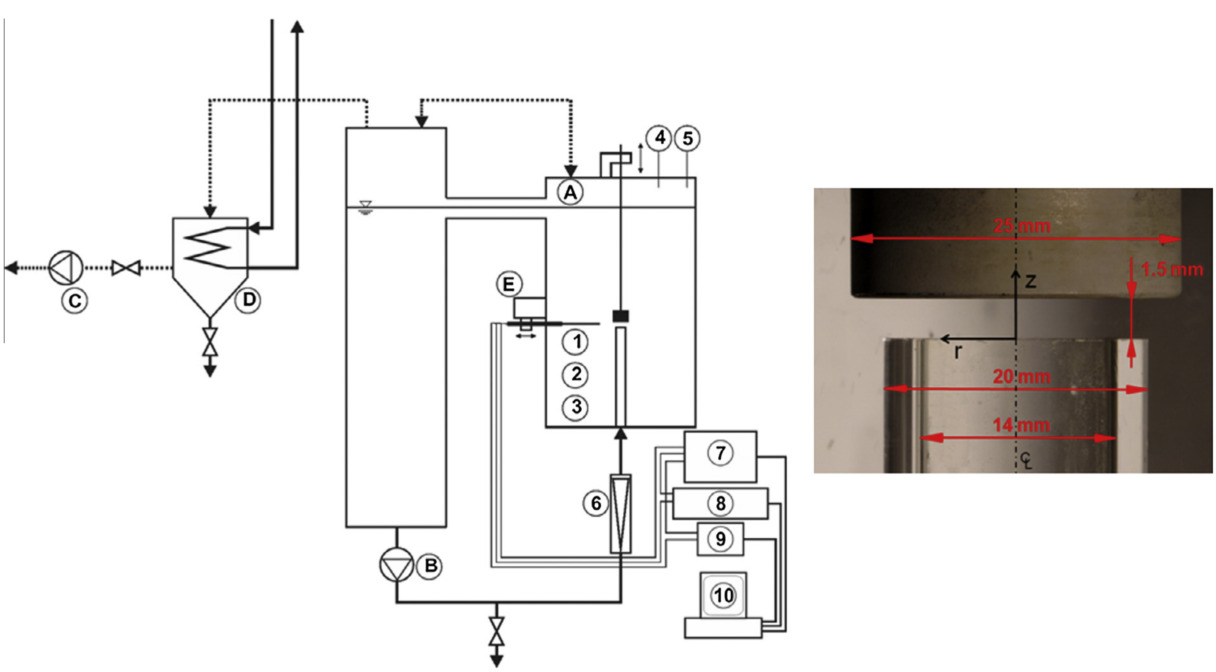

Fig. 1. Experimental set up. *Main parts*: vacuum chamber (A), circulation pump (B), vacuum pump (C), condenser (D), probe traversing system (E). *Measuring equipment*: double resistivity probe (1), optical pressure probe (2, optionally), CTA probe (3, optionally), digital thermometer (4), digital differential manometer (5), rotameter (6), DAQ card (7), pressure control unit (8), CTA system (9), PC (10).